THE JOURNAL OF BIOLOGICAL CHEMISTRY VOL. 291, NO. 20, pp. 10646–10658, May 13, 2016

The Role of PIWIL4, an Argonaute Family Protein, in Breast Cancer*[S]

Received for publication, February 22, 2016, and in revised form, March 7, 2016 Published, JBC Papers in Press, March 8, 2016, DOI 10.1074/jbc.M116.723239

Zifeng Wang[‡§1], **Na Liu**[¶‖2], **Shuo Shi**[§], **Sanhong Liu**[§3], **and Haifan Lin**[‡§¶‖4]

From the [‡]*School of Life Science and Technology and* [§]*Shanghai Institute of Advanced Immunochemical Studies, ShanghaiTech University, Shanghai 201210, China and the* [¶]*Yale Stem Cell Center and* [‖]*Department of Cell Biology, Yale University School of Medicine, New Haven, Connecticut 06520*

P-element-induced wimpy testis (PIWI) proteins bind to PIWI-interacting RNAs and play key roles in the biogenesis and functions of PIWI-interacting RNAs. It has been reported that PIWI proteins are essential for stem cell self-renewal and germline development in diverse organisms and that they are ectopically expressed in multiple forms of cancer. However, the role of PIWI in cancer remains elusive. Here we report that one of the four PIWI proteins in humans, PIWIL4, is highly expressed in both breast cancer tissues and the cytoplasm of MDA-MB-231 cells derived from breast cancer. Reducing PIWIL4 expression drastically impairs the migration ability of MDA-MB-231 cells, significantly increases their apoptosis, and mildly affects their proliferation. Our transcriptome and proteome analysis reveal that these functions are at least partially achieved via the PIWIL4 regulation of TGF-β and FGF signaling pathways and MHC class II proteins. These findings suggest that PIWIL4 may serve as a potential therapeutic target for breast cancer.

PIWI[5] proteins represent a subfamily of the Argonaute (Ago) protein family and are highly conserved among eukaryotes and archaea. PIWI proteins bind to a class of non-coding small RNAs called PIWI-interacting RNAs (piRNAs) (1–4). The PIWI-piRNA complex regulates gene expression at epigenetic and posttranscriptional levels (5–8). PIWI proteins and piRNAs are mostly expressed in the germ line, where PIWI proteins have been demonstrated to be essential for germ line development, stem cell self-renewal, and gametogenesis in diverse organisms (4, 9–14). In addition, there is increasing evidence for somatic expression of PIWI proteins in *Drosophila* and mouse tissues (14–16). Furthermore, it has been reported that PIWI proteins have aberrant and ectopic expression in a wide spectrum of cancers (17–23). For example, *PIWIl2* is highly expressed in breast cancer (24). Hence, PIWI might be involved in cancer formation and/or progression.

Breast cancer comprises four subtypes based on the expression of estrogen receptor, progesterone receptor, and human epidermal growth factor receptor (HER2). Triple-negative breast cancer (TNBC) lacks estrogen receptor, progesterone receptor, and HER2 expression (25–27), represents ~10–25% of all breast cancers, and is a clinical therapy hot spot because of the vulnerability of younger women to this subtype of breast cancer (28). Furthermore, TNBC patients do not benefit from targeted treatments such as endocrine therapy or trastuzumab because this subtype of cancer lacks the appropriate targets for these drugs. These challenges point to the pressing need to identify pathogenic pathways in TNBC. Recent studies have identified genetic alterations and gene expression profiles associated with subtypes of TNBC, including the implication of the PI3K/Akt/mTOR (mechanistic target of rapamycin) pathway in TNBC (29–32). However, therapeutic blockade of this pathway with the PI3K/Akt/mechanistic target of rapamycin inhibitor has not been effective, indicating the existence of other mechanisms that are determinative in inducing TNBC.

Here we report that PIWIL4 is widely expressed in breast cancer samples and several cell lines derived from TNBC. To explore the mechanisms involved in TNBC, we focused our study on using a cell line (MDA-MB-231) as a model in which PIWIL4 is expressed at the highest level. We show that reducing PIWIL4 expression significantly compromises cell migration, increases apoptosis, and reduces proliferation of the cells. These effects may be achieved at least in part by activating TGF-β, MAPK/ERK, and FGF signaling. In addition, PIWIL4 represses MHC class II expression, which might help cancer cells to avoid immune recognition and reaction.

Experimental Procedures

Cell Culture and Clinical Samples—MDA-MB-231, MDA-MB-435, MDA-MB-468, and MDA-MB-453 cells were cultured in L-15 medium (Leibovitz, Sigma, L1518-500ML) supplemented with 10% fetal bovine serum and incubated at 37 °C without CO_2. BT474 and 4T1 cells were cultured in RPMI 1640 medium (Life Technologies, 61870036) supplemented with 10% fetal bovine serum, and MCF-10A cells were cultured in MEBM medium (Lonza, CC-3151) supplemented with 10% bovine calf serum, and these three cell lines were incubated at 37 °C with 5% CO_2.

* This work was supported by the Shanghai Institute for Advanced Immunochemical Studies at ShanghaiTech University (to H. L.). The authors declare that they have no conflicts of interest with the contents of this article.

The nucleotide sequences reported in this paper have been submitted to the GEO database with accession number GSE78238.

[S] This article contains supplemental Figures S1–S4, Tables S1–S8, and Data S1.

[1] Supported by the School of Life Science and Technology at ShanghaiTech University.

[2] Supported by a Mathers Award (to H. L.).

[3] To whom correspondence may be addressed: Tel.: 203-785-6239; Fax: 203-785-4305; E-mail: haifan.lin@yale.edu.

[4] To whom correspondence may be addressed: Tel.: 86-21-2068-5133; E-mail: liush@shanghaitech.edu.cn.

[5] The abbreviations used are: PIWI, P-element-induced wimpy testis; piRNA, PIWI-interacting RNA; TNBC, triple-negative breast cancer; miRNA, microRNA.

20 pairs of clinical samples were purchased from the tissue bank of the Institute of Health Sciences, Chinese Academy of Sciences. The local ethics committee approved the study, and the regulations of this committee were followed.

RNA Extraction and Quantitative Real-time PCR—Total RNA was isolated using TRIzol (Invitrogen) according to the protocol of the manufacturer. For reverse transcription, we used 1 μg of RNA reverse transcriptase and the ABI high-capacity kit (Life Technologies, 4368814). Real-time PCR reactions were performed according to the protocol of the Bio-Rad real-time PCR system (iQ™ SYBR Green Supermix and CFX96™ real-time system). Primers of GAPDH were designed as the real-time PCR control. Quantitative PCR primers are listed in supplemental Table S1 (33, 34).

PIWIL4 cDNA Cloning—The PIWL4 cDNA primers were designed as follows: forward, 5′-CGCGGATCCATGAGTGGAAGAGCCCG-3′; reverse, 5′-CGCGGATCCTCACAGGTAGAAGAGATGG-3′. Total RNA was used for cDNA synthesis by SuperScript® III reverse transcriptase (Invitrogen, 18080044) according to the protocol of the manufacturer. The cDNA was used as a template for amplification by Phusion high-fidelity DNA polymerase (New England Biolabs, M0530L) in PCR and cloned into the pMDTM19-T vector by a cloning kit (Takara, 6013).

Western Blotting Analysis—Total proteins were extracted by radioimmunoprecipitation assay buffer (Santa Cruz Biotechnology, sc-24948) according to the protocol of the manufacturer. Samples were mixed (3:1) with 4× protein SDS-PAGE loading buffer (Takara, 9173) and heated at 100 °C for 10 min. The human testicular total protein lysate was purchased from Clontech (catalog no. 635309). 30 μg of protein was resolved by the TGX Fast Cast acrylamide kit, 7.5% or 10% (Bio-Rad, 1610173TA) at 120 V, and electrotransferred to a PVDF membrane (Merck/Millipore, IPVH00010) at 0.3A for 1.5 h. The membrane was blocked with 5% Difco™ skim milk (BD Biosciences, 232100) at room temperature for 2 h, which was diluted with TBS (Bio-Rad, 1706435) supplemented with 0.1% Tween 20 (Santa Cruz Biotechnology, sc-29113). PIWIL4 antibody (Abcam, ab111714) was used at 1:1000 dilution. N-cadherin antibody (Abcam, ab18203) at 1:1000 dilution, E-cadherin (Cell Signaling Technology, 3195S) at 1:1000 dilution, cleaved caspase-3 (Cell Signaling Technology, 9664) at 1:1000 dilution, p27 Kip1 (D69C12) XP® rabbit mAb (Cell Signaling Technology, 3686) at 1:1000 dilution, phospho-Smad (Ser-465/467) antibody (Cell Signaling Technology, 3101) at 1:1000 dilution, and β-Actin antibody (Cell Signaling Technology, 4970S) at 1:1000 dilution were used. A cell cycle/checkpoint antibody sampler kit (Cell Signaling Technology, 9917) was used for detecting cell cycle-dependent phosphorylation of CDC2 and CHK2.

PIWIL4 shRNA Knockdown Analysis—RNAi vector pSUPER-puro was purchased from Promega. Three short hairpin DNA sequences were designed as in supplemental Table S1. The DNA sense and antisense sequences were annealed in a pairwise fashion and cloned into the pSUPER-puro vector.

MDA-MB-231 cells were transfected with Lipofectamine 2000 (Life Technologies, 11668019) according to the instructions of the manufacturer. Transfected cells were selected using 0.8 μg/ml puromycin. The silencing effect on the PIWIL4 gene was assessed by quantitative PCR and Western blotting analysis according to the aforementioned protocols.

Nuclear-Cytoplasmic Fractionation—Approximately 10^6 cells were washed with PBS twice, followed by centrifugation at 1000 × *g* for 3 min. The resulting supernatant was discarded. The pellet was added to 150–200 μl of buffer B (10 mM Hepes, 10 mM KCl, 2 mM $MgCl_2$, 0.1 mM EDTA, 0.2% Nonidet P-40, protease inhibitor, and 1 mM DTT), incubated on ice for 30 min, and centrifuged at 4 °C at 13,200 rpm for 6 min. Cytoplasmic proteins were collected as the supernatant to new tubes and stored at −80 °C until use. The nuclear pellet was washed with 500 μl of wash buffer (10 mM Hepes, 20 mM KCl, 2 mM $MgCl_2$, 0.1 mM EDTA, protease inhibitor, and 1 mM DTT) and centrifuged at 4 °C at 3000 rpm for 5 min. The supernatant was discarded, and the nuclear pellet was dissolved in 50–80 μl of extraction buffer (20 mM Hepes, 0.64 mM NaCl, 1.5 mM $MgCl_2$, 0.2 mM EDTA, 2.5% glycerol, protease inhibitor, and 1 mM DTT), vortexed for 15 s, incubated on ice for 30 min, vortexed for 10–15 s at 10-min intervals, and centrifuged at 4 °C and 13,200 rpm for 20 min. The supernatants, which contained nucleus proteins, were collected in new tubes and stored at −80 °C for later use. Separation of the cytoplasmic and nuclear fractions was verified by Western blotting for β-tubulin and TBP (Cell Signaling Technology, anti-β-tubulin and anti-TBP antibody).

Apoptosis Assay—We stained cancer cells with the FITC Annexin V apoptosis detection kit I (BD Biosciences, 556547) according to the protocol of the manufacturer and analyzed early- and late-stage apoptosis by FACS (FACS Aria™ IIII, BD Biosciences).

Cell Death and Cell Proliferation Assays—Cells were mixed (1:1) with trypan blue solution, 0.4% (Gibco, 15250061), 10 μl of which was seeded on Countess chamber slides (Invitrogen, C10312) and counted with a Countess™ automated cell counter (Invitrogen, C10227). 2×10^3 cells/well were seeded in 96-well cell culture plates and 6-cm^2 dishes. Each sample had three repeats. Cell proliferation was determined using CellTiter 96® AQueous MTS (3-(4,5-dimethylthiazol-2-yl)-5-(3-carboxymethoxyphenyl)-2-(4-sulfophenyl)-2*H*-tetrazolium, inner salt) reagent powder (Promega, G1111) according to the instructions of the manufacturer. Absorbance at 490-nm wavelength was read using EnSpire® multimode plate readers (PerkinElmer Life Sciences), and clone formation was visualized by staining with crystal violet solution (Beyotime Biotechnology, C0121).

Wound Healing and Transwell Migration Assays—5×10^4 cells were seeded in a 96-well plate, and a wound was introduced with a wound maker kit (Essen Bioscience). Wounded monolayers were washed twice with PBS to remove non-adherent cells. Cells were cultured in 2% FBS for 48 h, and the wound healing tracks were recorded with an IncuCyte® Zoom live-cell analysis system (Essen Bioscience). The transwell assay was done using Corning FluoroBlok™ cell culture inserts (Falcon, 351152) according to the protocol of the manufacturer.

Immunofluorescence Microscopy—2×10^5 cells were seeded on a coverslip (Fisherbrand, 12-545-83) in a 24-well plate. After 24 h, cells were washed three times in 1× PBST (1% Tween 20

in phosphate-buffered saline, 5 min each time), fixed in 4% formaldehyde (paraformaldehyde powder, 95%, 158127-2.5KG, Sigma) at room temperature for 15 min, incubated with 0.1% Triton X-100 (Santa Cruz Biotechnology, sc-29112) at room temperature for 15 min, washed in PBST three times (5 min each wash), blocked in 3% BSA at room temperature for 2 h, and washed in TBST again for 5 min. The cells were incubated with anti-PIWIL4 (Abcam, ab111714, 1:500 dilution) and anti-hDcp1a (56-Y) antibodies (Santa Cruz Biotechnology, sc-100706, 1:500 dilution) in 3% BSA at 4 °C overnight with no primary antibody addition as a negative control. After incubation, cells were washed three times in 1× PBST, 5 min each time. FITC-conjugated AffiniPure goat anti-mouse IgG and IgM (heavy and light chain) (Jackson ImmunoResearch Laboratories, 115-095-044, 1:100 dilution) or Alexa Fluor 594-conjugated AffiniPure goat anti-rabbit IgG, Fc fragment-specific (Jackson ImmunoResearch Laboratories, 111-585-008, 1:500 dilution) were added and incubated at room temperature for 2 h, followed by a PBST wash once for 5 min. DAPI (Life Technologies, D1306, 1:5000 dilution) was then added to the PBST buffer and incubated at room temperature for10 min, followed by three washes in PBST, 5 min each time. Coverslips were removed one at a time, and we added 1 drop of FluorPreserve™ (Merck/Millipore, 345787-25MLCN), mounted them to the glass slide, pressed gently, sealed them with nail polish, and stored them at 4 °C overnight before confocal immunofluorescence microscopy (Zeiss, LSM710).

Mass Spectrometry and RNA Deep Sequencing—10^6 MDA-MB-231 cells or cells treated with shPIWIL4–1, shPIWIL4–2, or shPIWIL4–3 were collected, lysed in 200 μl of SDT lysis buffer (4% (w/v) SDS, 100 mM Tris/HCl (pH 7.6), and 0.1 M DTT), and then incubated at 95 °C for 3–5 min. Filter-aided proteome preparation was carried out according to the protocol detailed in supplemental Data 1 and sequenced by Thermo Scientific Fusion with EASY-nLC 1000.

For RNA sequencing, ~10^6 MDA-MB-231 cells with or without shPIWIL4–3 treatment were collected. Total RNA was isolated using TRIzol (Invitrogen, 15596026) according to the protocol of the manufacturer. mRNAs and small RNAs were sequenced with an Illumina HiSeq3000 platform (Jing Neng Co., Shanghai, China). HTSeq software was used for the statistics of the original mRNA deep sequencing data of the control and shPIWIL4–3-treated samples. DESeq software was used to screen differentially expressed genes compared with the control ($p \leq 0.05$ or -fold change ≥ 2).

Gene Ontology and Pathway Analysis—A gene ontology and pathway analysis was conducted using an online tool. Gene ontology level 2 and 3 categories were selected for mRNA sequencing and mass spectrometry analysis, respectively.

Genome Mapping—The small RNA sequences were generated with Illumina HiSeq3000, and we trimmed off linkers with the FASTX toolkit. We selected sequences with sizes ranging from 12–43 nucleotides for analysis. The reference genome was human genome hg38. The gene annotation information was based on the Ensembl annotation. The miRNA annotation was based on version 21 of miRBase. Repeats and transposon annotation were based on RepeatMasker. Complete rRNA references were from the NCBI. One mismatch was allowed for mapping sequences against rRNA, tRNA, small nucleolar RNA, and small nuclear RNA.

Identification of Known piRNAs—Human known piRNAs in piRNABank and piRBase served as references to identify known piRNAs. Only the small RNAs that had an identical sequence to these reference piRNA sequences were defined as known piRNAs.

Effect of PIWIL4 Knockdown on Known piRNAs—The abundance of piRNAs was scaled according to the total mapped reads for comparison across different conditions. The shPIWIL4 treated-to-nontreated control ratio was calculated to measure the effect of PIWIL4 knockdown on piRNAs. In total, we detected ~200 small RNAs annotated as piRNAs in piRNABank and piRBase, of which ~20 were affected (fold change ≥ 2 or $\leq$ ½) when PIWIL4 was knocked down.

Results

The PIWIL4 Gene Is Highly Expressed in both Breast Cell Lines and Breast Cancer Samples—It has been reported that PIWI proteins have aberrant and ectopic expression in cancers, such as the expression of PIWIL2 in breast cancer (17–22, 35). Because all PIWI proteins are necessary for germ line development and stem cell self-renewal, we systematically examined the expression of three known active *PIWI* genes in humans, *piwil1*, *piwil2*, and *piwil4*, in six different types of human breast cancer cell lines and 20 pairs of normal and breast cancer samples from 20 patients by quantitative RT-PCR (Fig. 1). *piwil1* and *piwil2* are expressed in four and two cell lines, respectively, at significantly higher levels than in a normal breast cell line (MCF-10A, a physiologically negative control) or a mouse breast cancer line (4T1, Fig. 1, *A* and *B*), consistent with a previous report of *PIWIL2* expression in breast cancer cells (35). In addition, *PIWIL1* is expressed at significantly higher levels compared with the normal tissue controls in two of 20 breast cancer samples (Fig. 1*D*). *PIWIL2* is more highly expressed than *PIWIL1* in one cancer cell line, MDA-MB-231 (Fig. 1*B*), and four of 20 breast cancer samples (Fig. 1*E*). Remarkably, *PIWIL4* is expressed at very high levels in five of six cancer cell lines, much higher than *PIWIL1* and *PIWIL2* (Fig. 1*C*). Furthermore, *PIWIL4* is significantly expressed in nine of 20 breast cancer samples, with five samples displaying a more than 50-fold up-regulation (Fig. 1*F*). This indicates that, among the three *PIWI* genes known to be active, *PIWIL4* has the best correlation with breast cancer.

To further establish a functional correlation between the expression of PIWI proteins and breast cancer, we analyzed a cancer genomics data bank, cBioPortal (36, 37). Our analysis showed that all three human *PIWI* genes have genetic alterations in breast cancer. We found that 2%, 7%, and 2% of breast patients cancer patients have amplification, deletion, missense mutation, and truncation of *PIWIL1*, *PIWIL2*, and *PIWIL4*, respectively (supplemental Fig. S1). Moreover, 2%, 2%, and 4% of *PIWIL1*, *PIWL2*, and *PIWIL4* patients have mRNA up-regulation (supplemental Fig. S1). When only considering TNBC patients, the percentage is increased to 11% ($n = 82$). The 4% of PIWIL4-positive patients is apparently lower than the 9% of 20 patients who we examined directly. This could be due to inherently lower sensitivity associated with surveying the expression of many genes in more than 5000 tumor samples from 20 can-

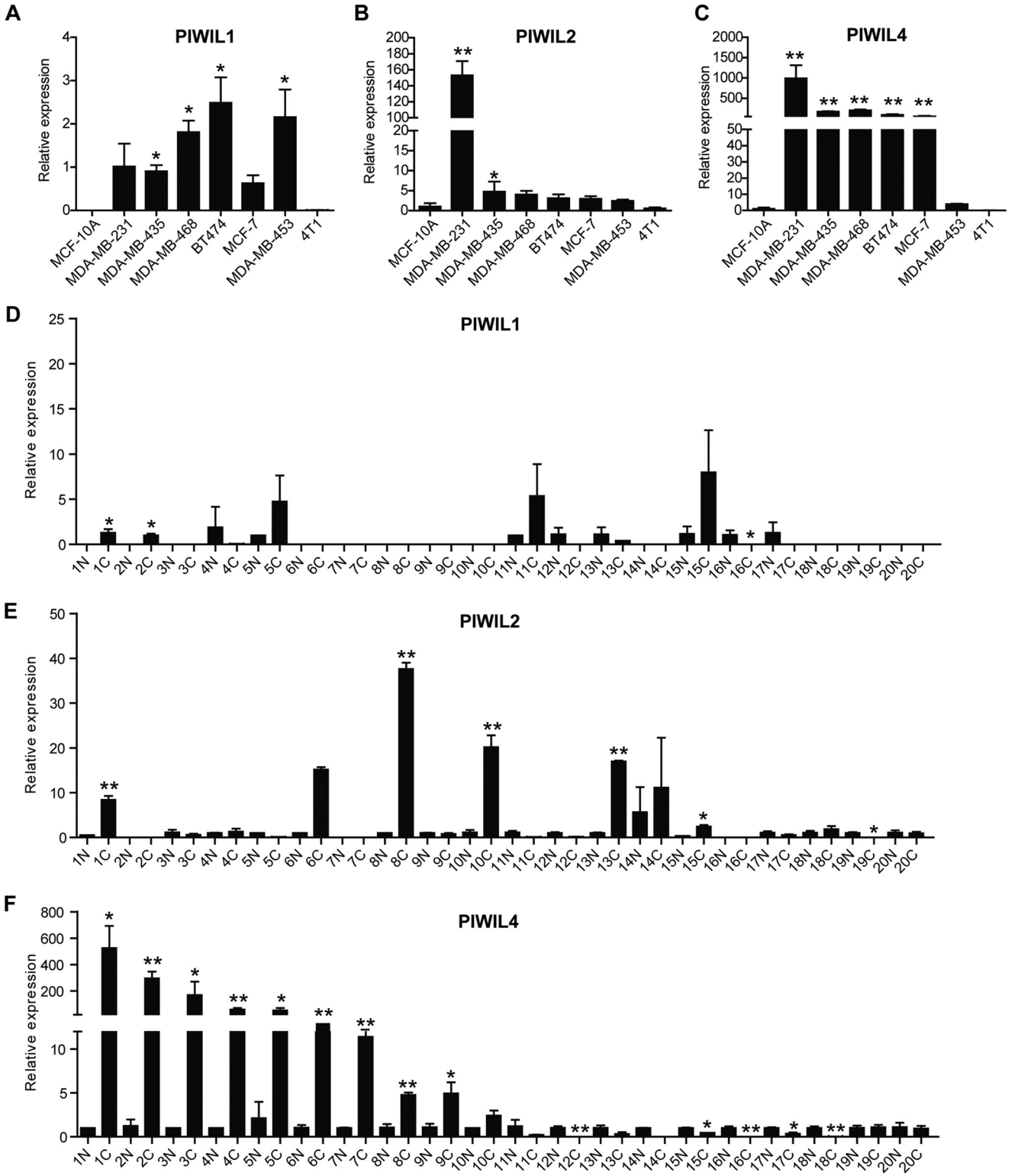

FIGURE 1. **PIWIL4 is widely highly expressed in TNBCs.** *A–C*, expression of PIWIL1 (*A*), PIWIL2 (*B*), and PIWIL4 (*C*) in seven breast cancer cell lines and a noncancerous breast cell line, MCF-10A. *D–F*, expression of PIWIL1 (*D*), PIWIL2 (*E*), and PIWIL4 (*F*) in 20 pairs of breast cancer samples (*C*) and their paired normal samples (*N*). *, $p < 0.05$; **, $p < 0.01$ compared with the controls.

cer studies. Alternatively, it could also reflect that 20 patients is a small sample size.

To investigate further correlation between PIWIL4 and breast cancer, we conducted a Kaplan-Meier survival analysis based on clinical data from a bioinformatics website, including 351–1616 patients for each analysis. Patients who have the upper tertile level of *PIWIL4* expression have lower overall survival, distance metastasis-free survival, and post-progression survival than patients with the lower 67% of *PIWIL4* expression (Fig. 2). This analysis further correlates *PIWIL4* to breast cancer.

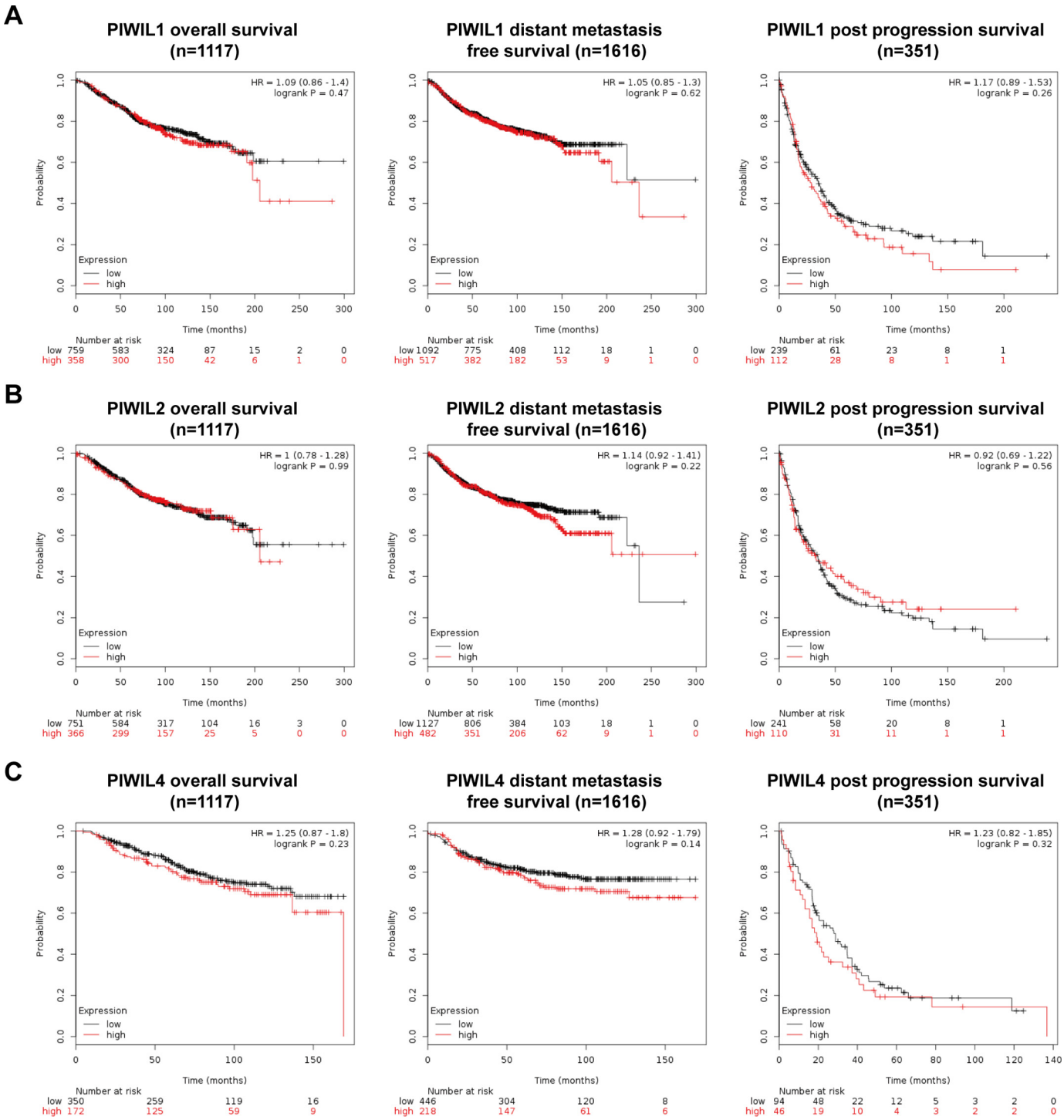

FIGURE 2. **PIWIL4 expression is highly correlated with breast cancer fatality and distant metastasis fatality.** *A–C*, clinical overall survival and distant metastasis-free and post-progression survival of breast cancer patients with the top *versus* the lower two tertile (labeled *high* and *low*, respectively) expression levels of PIWIL1 (*A*), PIWIL2 (*B*), and PIWIL4 (*C*). The data resource was the KM-plotter database. *P*, log-rank *p*; *HR*, hazard ratio.

The PIWIL4 Protein Is Localized in the Cytoplasm and Exists in Multiple Isoforms in MDA-MB-231 Cells—To further investigate the role of PIWIL4 in breast cancer, we examined its expression and subcellular localization in MDA-MB-231 cells. We separated the cytoplasmic and nuclear fractions of the cell lysate from MDA-MB-231 cells (WT), MDA-MB-231 cells transfected with an empty plasmid vector (*Con*), and MDA-MB-231 cells transfected with a *PIWIL4*-overexpressing construct in the vector (*OE*) by centrifugation, followed by Western blotting, which revealed that PIWIL4 is present in the cytoplasm (Fig. 3*A*). Immunofluorescence microscopy results confirmed that PIWIL4 is present in the cytoplasm and further showed that it is not co-localized with the P body (Fig. 3*B*). Surprisingly, not all MDA-MB-231 cells showed a PIWIL4 signal when stained with anti-PIWIL4 antibody against 639 – 839 amino acid residues (in exons 15–20) of PIWIL4 (Fig. 3, *B* and

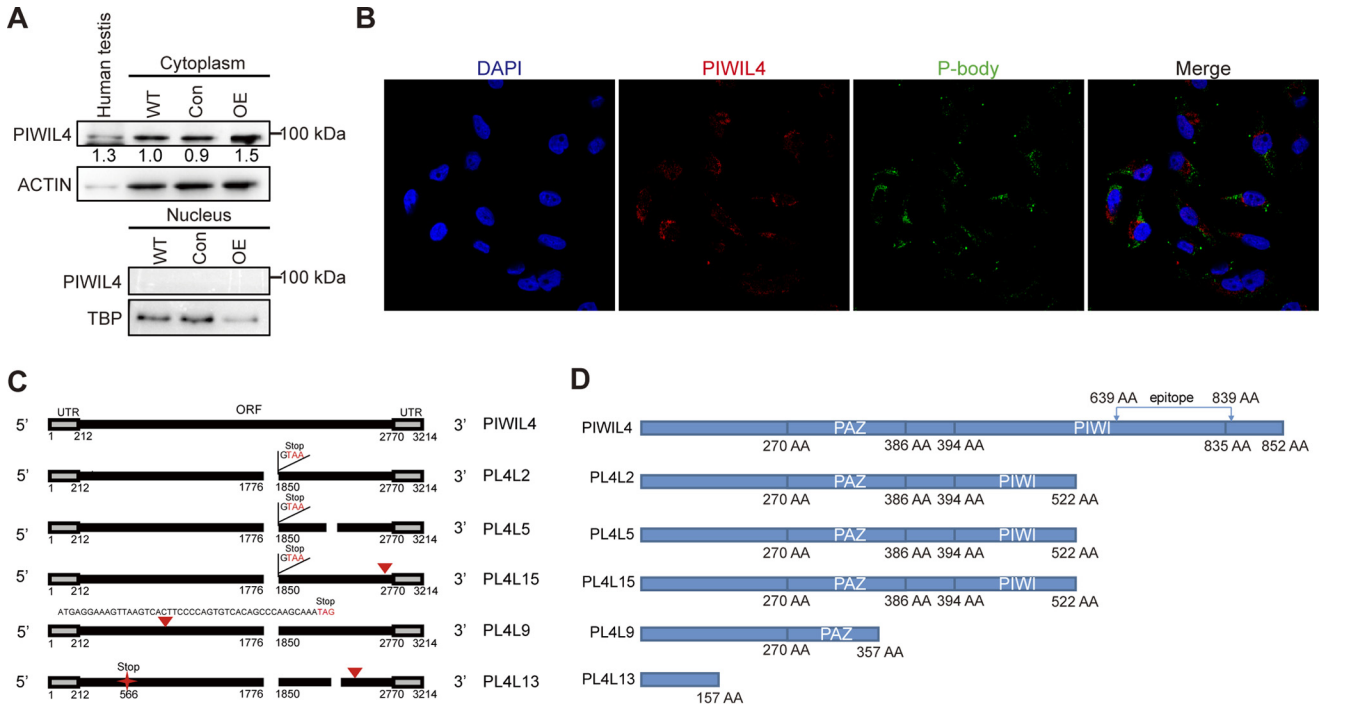

FIGURE 3. **PIWIL4 is localized in the cytoplasm and exists in multiple isoforms in MDA-MB-231 cells.** *A*, expression of PIWIL4 in the cytoplasm and nucleus of MDA-MB-231 cells, as indicated by subcellular fractionation and Western blotting analysis, in which Actin and TBP were used as cytoplasmic and nuclear markers, respectively. *Con*, control MDA-MB-231 cells transfected with an empty plasmid; *OE*, MDA-MB-231 cells with PIWIL4 overexpression via transfection. *B*, immunofluorescence staining of PIWIL4 and hDcp1a (a P body marker) in MDA-MB-231 cells. *C*, six PIWIL4 mRNA isoforms of PIWIL4 in MDA-MB-231 cells, with deletions, insertions, and stop codons indicated. PIWIL4 is the wild-type, full-length isoform. PL4L9 has a portion of intron inserted before exon 9. PL4L13 has a cytosine C deletion in the 566 site (*red star*). The insert sequence in PL4L13 is 5′-GTACTAAAAATATAGCAATGTGGGTGGGCTCCAAGGACTGTTCCTTCAG-ACCTCAAATCCACATGCTTATAGAAGACCACATAG-3′. The insert sequence in PL4L15 is 5′-GCCAAGAGCTGTTCCCAAAGGCCAAGCCCAAGGTTTGCACGAAGCT-CCTCCAAGGAGTTCCAAACTTGAGATCACAGGACAAAGACTAGTCTGAAGTGTGATGGCTCCCTACTCCCAGCACCATGAAGCCAGAGTGACTTTTCACTCCATCCTC-CCCAGTGAGCTTAAGTTCCCA-3′. The lessons in other isoforms are self-evident from the figure. *D*, four PIWIL4 protein isoforms corresponding to the six mRNA isoforms. *AA*, amino acids.

D, and supplemental Fig. S2). This indicates that these cells either do not express PIWIL4 or express aberrant PIWIL4 isoforms that lack 639–839 amino acid residues. To discriminate between these two possibilities, we reverse-transcribed PIWIL4 mRNAs isolated from MDA-MB-231 cells and sequenced the resulting cDNAs. These analyses revealed that there are five variants of PIWIL4 transcripts in MDA-MB-231 cells (Fig. 3*C*). All of the variants have deletions or insertions that cause premature termination before the 639–839 amino acid residues of PIWIL4 (Fig. 3*D*). The inserted sequences in PL4L9, PL4L13, and PL4L15 are all intron sequences of the *PIWIL4* gene. Correspondingly, there are three aberrant PIWIL4 protein isoforms (Fig. 3*D*). These observations indicate the instability of the MDA-MB-231 genome, which is a typical situation in many cancer cell lines.

PIWIL4 Inhibits MDA-MB-231 Cell Apoptosis and Promotes Migration—To reveal the effect of ectopic PIWIL4 expression in cancer cells, we knocked down PIWIL4 expression using the pSuper-shRNA knockdown system with three different shRNA sequences against *PIWIL4* mRNA and analyzed the effect of the knockdowns on the function of MDA-MB-231 cells. Fig. 4*A* indicates the three shRNA-corresponding regions in *PIWIL4* mRNA (at the exon 2-exon 3 junction, exon 7, and exon 17, respectively). All of these three shRNAs effectively reduced both *PIWIL4* mRNA and PIWIL4 protein levels (Fig. 4*B*). Reduction of PIWIL4 weakly inhibited cell proliferation (Fig. 4*C*) and colony formation ability (Fig. 4*D*) but caused significantly increased apoptosis (Fig. 4*F*). Correspondingly, we found that PIWIL4 knockdown increased the levels of phosphorylated CHK2 and phosphorylated CDC2 (two G_2 phase checkpoint markers) and p27 (a cell proliferation marker) and drastically increased the level of cleaved caspase 3, an indicator of the activation of the caspase 3 pathway (Fig. 4*E*). These results validated the negative impact of PIWL4 knockdown on cancer cell survival.

To explore whether PIWIL4 also has a role in the migration and metastasis of cancer cells, we first conducted the *in vitro* wound healing assay (*i.e.* the scratch assay) and the transwell migration assay on MDA-MB-231 cells. Knocking down PIWIL4 with each of the three anti-*PIWIL4* shRNAs significantly inhibited the migration ability of these cells by either the scratch assay (Fig. 4*G*) or the transwell assay (Fig. 4*H*). These results indicate that PIWIL4 promotes the migratory ability of MDA-MB-231 cells.

To further investigate whether the PIWIL4-dependent migratory ability of MDA-MB-231 cells reflects their epithelial-to-mesenchymal transition, we examined the expression of a key epithelial marker, E-cadherin, and a key mesenchymal marker, N-cadherin, in MDA-MB-231 cells by Western blotting analysis. These cells normally express only N-cadherin but not E-cadherin (Fig. 4*E*), indicating that these cancer cells have acquired the mesenchymal fate. Remarkably, knocking down PIWIL4 abolished N-cadherin expression but induced strong expression of E-cadherin (Fig. 4*E*). These data indicate that the

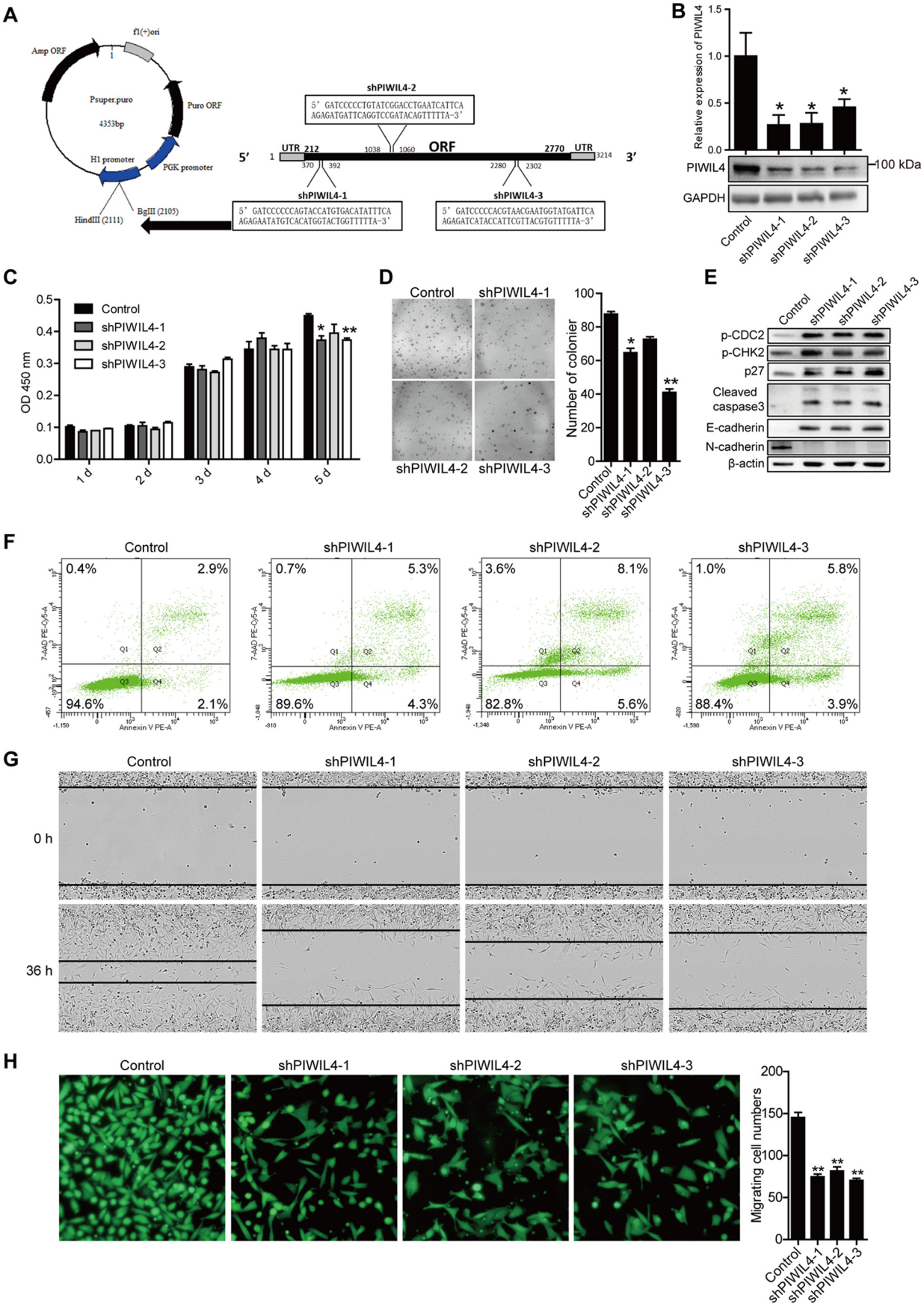
A
f1(+)ori
Amp ORF
Psuper.puro
4353bp
Puro ORF
H1 promoter
PGK promoter
HindIII (2111)
BglII (2105)
shPIWIL4-2
5' GATCCCCCTGTATCGGACCTGAATCATTCA
AGAGATGATTCAGGTCCGATACAGTTTTTA-3'
5'
UTR 212
1038
1060
ORF
2770
UTR
3214
3'
370
392
2280
2302
shPIWIL4-1
5' GATCCCCCCAGTACCATGTGACATATTTCA
AGAGAATATGTCACATGGTACTGGTTTTTA-3'
shPIWIL4-3
5' GATCCCCCACGTAACGAATGGTATGATTCA
AGAGATCATACCATTCGTTACGTGTTTTTA-3'
B
Relative expression of PIWIL4
PIWIL4
100 kDa
GAPDH
Control
shPIWIL4-1
shPIWIL4-2
shPIWIL4-3
C
OD 450 nm
Control
shPIWIL4-1
shPIWIL4-2
shPIWIL4-3
1 d
2 d
3 d
4 d
5 d
D
Control
shPIWIL4-1
shPIWIL4-2
shPIWIL4-3
Number of colonier
E
p-CDC2
p-CHK2
p27
Cleaved caspase3
E-cadherin
N-cadherin
β-actin
F
Control
shPIWIL4-1
shPIWIL4-2
shPIWIL4-3
0.4%
2.9%
94.6%
2.1%
0.7%
5.3%
89.6%
4.3%
3.6%
8.1%
82.8%
5.6%
1.0%
5.8%
88.4%
3.9%
7-AAD PE-Cy5-A
Annexin V PE-A
G
Control
shPIWIL4-1
shPIWIL4-2
shPIWIL4-3
0 h
36 h
H
Control
shPIWIL4-1
shPIWIL4-2
shPIWIL4-3
Migrating cell numbers

PIWIL4-deficient MDA-MB-231 cells have abandoned the mesenchymal fate and have reacquired key features of the epithelial fate. Therefore, PIWIL4 is required for the epithelial-to-mesenchymal transition and acquisition of the migratory ability of MDA-MB-231 cells.

PIWIL4 Activates TGF-β and FGF Signaling in MDA-MB-231 Cells—To investigate the molecular mechanism underlying PIWIL4 function in MDA-MB-231 cancer cells, we examined the transcriptome and proteome of MDA-MB-231 cells with and without *shPIWIL4–3* knockdown by deep sequencing of mRNAs and mass spectrometry of total cellular lysate, respectively. We found that, among 26,057 mRNAs that can be detected by at least one read in MDA-MB-231 cells via deep sequencing, 332 mRNAs were significantly down-regulated but 400 mRNAs were up-regulated when PIWIL4 was knocked down, as summarized in the heat map in Fig. 5*A*. The 60 most up- and down-regulated genes (38 up-regulated and 22 down-regulated) are shown with names in Fig. 5*B*.

To detect the impact of PIWIL4 knockdown on the cellular protein profile, we conducted mass spectrometry analyses of MDA-MB-231 cells and MDA-MB-231 cells with PIWIL4 knocked down by the three different shRNAs. The three PIWIL4 knockdown samples show nicely overlapping protein profiles (49.74% overlap between *shPIWIL4–1* and *shPIWIL4–2*, 50.41% overlap between *shPIWIL4–1* and *shPIWIL4–3*, 50.98% overlap between *shPIWIL4–2* and *shPIWIL4–3*, and 36.47% were found in all three samples), with 2571 proteins detected in all three PIWIL4 knockdown samples (Fig. 5*C*). Of the 2571 proteins, 2364 proteins were also present in MDA-MB-231 cells without PIWIL4 knockdown. Only 207 proteins were not detected in normal cancer cells. This suggests that reducing PIWIL4 expression does not significantly activate the expression of new proteins. However, 1288 proteins were not detectable in any of the three PIWIL4 knockdown samples. This indicates that PIWIL4 promotes the expression of many proteins in MDA-MB-231 cancer cells.

To investigate which mRNAs are down-regulated and which proteins become undetected under the PIWIL4 deficiency condition, we conducted a pathway enrichment analysis of the 332 most down-regulated mRNAs and the 1288 proteins that are only detected in MDA-MB-231 cancer cells without PIWIL4 knockdown. These analyses showed that MAPK-ERK, TGF-β, and FGF were the most enriched pathways (Fig. 5*E* and supplemental Fig. S4*A*). Full lists are shown in supplemental Tables S2 and S3 and include TGFβR1, TGFβR2, FGFR2, TGFβ1, and TGFβ3, which are no longer detectable in the three PIWIL4 knockdown samples.

To validate the down-regulation of the above proteins, we measure the mRNA expression of TGFβR1, TGFβR2, FGFR2, TGFβ1, and TGFβ3 by quantitative RT-PCR. Indeed, all of the five genes were down-regulated in all three different PIWIL4 knockdown cell samples (Fig. 5*F*). The down-regulation of the TGF pathway components is further supported by gene ontology analysis of 1288 proteins specifically present in normal cancer cells and 207 proteins specifically present in PIWIL4 knockdown cells (totally 1495 proteins), which showed that the most enriched gene ontology term is transferase activity and transferring phosphorus-containing groups (Fig. 5*G*), which is frequently involved in protein activity, including the TGF-β, FGF, and MAPK-ERK signaling pathways. Supplemental Fig. S3 shows the most significantly enriched biological processes, cellular components, and molecular functions as ranked by their *p* values, which reveals that cell division is also an enriched biological process (the full list is presented in supplemental Table S4). Taken together, we conclude that PIWIL4 promotes MDA-MB-231 epithelial-to-mesenchymal transition, migratory ability, and proliferation and inhibited apoptosis partially by activating the TGF-β and FGF signaling pathways.

PIWIL4 Represses the Expression of MHC II Genes in MDA-MB-231—Tumorigenesis and development is a complex process involving not only cell proliferation but also tumor immune escape pathways. Combined gene ontology analysis of the 400 up-regulated mRNAs and 332 down-regulated mRNAs (total of 732 genes) revealed that genes related to tumor immune escape were enriched among the 62 gene ontology terms (supplemental Table S5). Especially the top 10 gene ontology terms are more related to cell adhesion, cell periphery, extracellular matrix structural constituents, single-multicellular organism cellular processes, and anatomical structure development (supplemental Fig. S4*C*). Supplemental Fig. S4, *D–F*, shows the top 10 most significant biological processes, cellular components, and molecular functions, respectively. Immunoresponse and cell adhesion are enriched among biological process, and the enriched molecules are mostly localized to the cell periphery, extracellular space, and cell surface, performing their roles of extracellular matrix structural constituent, antigen binding, and receptor binding. Moreover, cell proliferation and death are also in the enriched terms. Pathway enrichment analysis of the 400 up-regulated genes reveals that PIWIL4 represses the expression of MHC class II mRNAs, including HLA-DRα, HLA-DPα1, HLA-DOα, HLA-DPβ1, cathepsin S, cathepsin E, dynamin 1, and CD74. This might lead to the up-regulation of some immune responses involved in the neuronal cell adhesion molecule, the signal regulatory protein family, and the cGMP pathway, as evident in supplemental Fig. S4B (a full list is presented in supplemental Table S6). These observations are consistent with the enrichment of translation-related mechanisms among the 207 most up-regulated proteins under the PIWIL4 deficiency condition (Fig. 5*D*, a full list is presented in supplemental Table S7). These results imply that PIWIL4

FIGURE 4. **PIWIL4 inhibits MDA-MB-231 cell apoptosis and promotes migration.** *A*, diagram of the pSuper-shRNA knockdown system with three sense shRNA sequences of PIWIL4. *PGK*, phosphoglycerate kinase. *B*, the mRNA level and protein level of MDA-MB-231 cells transfected with shPIWIL4–1, -2, and -3 and shCon (an empty vector control) for 48 h. *C*, growth curve of MDA-MB-231 cells with shPIWIL4–1, -2, and -3 and shCon. *OD*, optical density. *D*, clone formation assay of MDA-MB-231 cells expressing shCon or shPIWIL4–1, -2, and -3. Colonies were counted after 10 days, indicating that PIWIL4 knockdown reduced the colony formation ability by up to 2-fold. *E*, protein levels of phosphorylated CHK2 and phosphorylated CDC2, p27, E-cadherin, N-cadherin, and cleaved caspase 3 in MDA-MB-231 cells expressing shCon and shPIWIL4. *F*, flow cytometry analysis of cell apoptosis using Annexin V and 7-amino-actinomycin D (*7AAD*) as early and late apoptotic markers, respectively. *G*, scratch assay indicating the wound healing results (*i.e.* migratory ability) of MDA-MB-231 cells transfected with shCon and shPIWIL4–1, -2, and -3. *H*, transwell assay of MDA-MB-231 cells expressing shCon or shPIWIL4–1, -2, and -3, showing that PIWIL4 knockdown significantly hampered cell migration. *, $p < 0.05$; **, $p < 0.01$ compared with the controls.

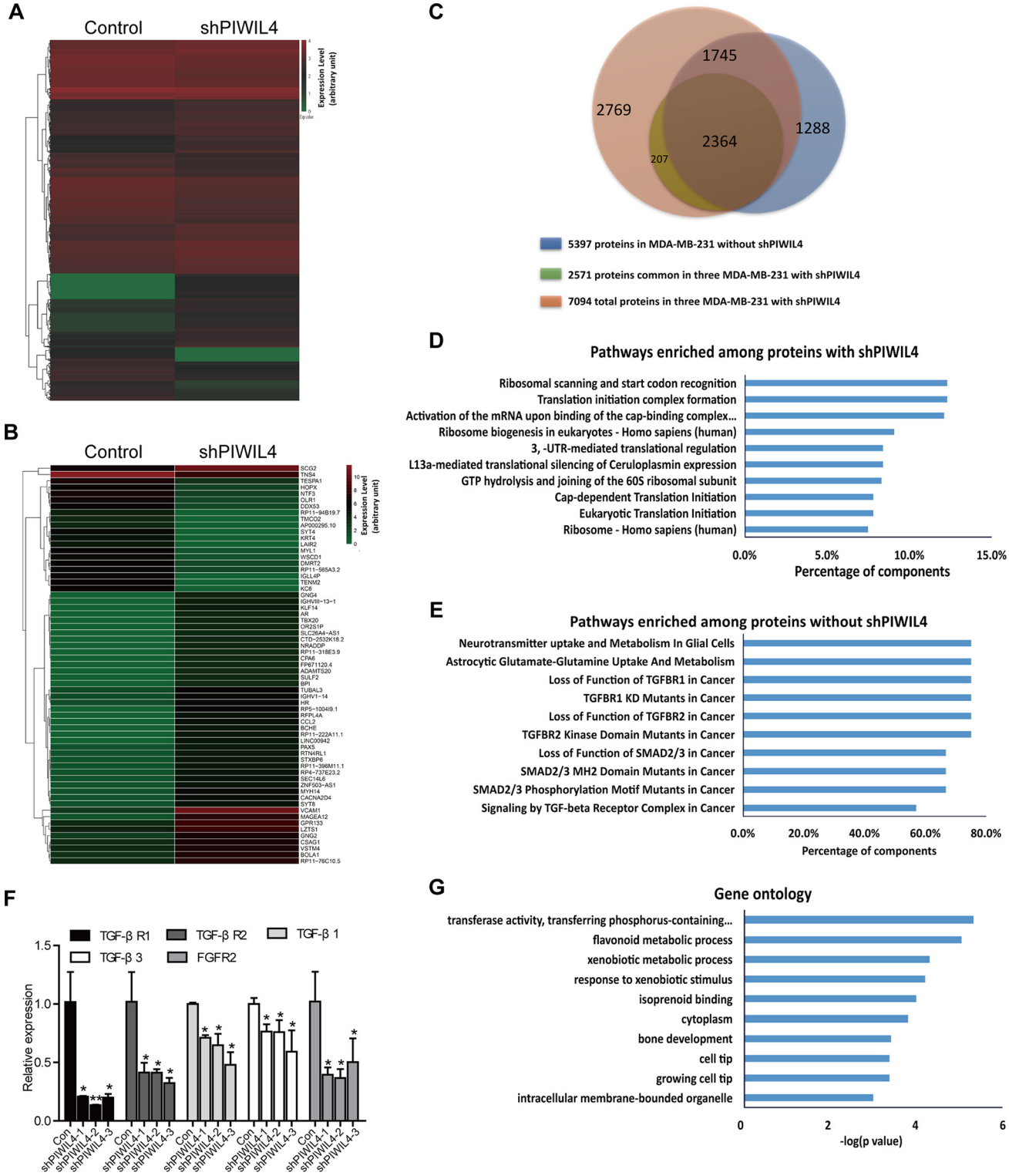

FIGURE 5. **PIWIL4 is essential for activation of TGF-β and FGF signaling in MDA-MB-231 cells.** *A*, heat map of 732 differentially expressed mRNAs between MDA-MB-231 cells with and without shPIWIL4–3 treatment. *Green* labeled *0* indicates the lowest expression level, *red* labeled *4* indicates the highest expression level, and the index was an arbitrary unit. B, heat map of the 60 most differentially expressed mRNAs between MDA-MB-231 cells with and without shPIWIL4–3 treatment. *C*, Venn diagram of three different PIWIL4 knockdown samples and control MDA-MB-231 cells. The *blue circle* (also appears in other colors because of the overlap with the *green* and *tan circles*) indicates 5397 proteins detected in MDA-MD-231 cells treated with shRNA vector only. The *green circle* (which appears as *dark tan* (207) and *dark brown* because of the overlap with the *blue* and *tan circles*) indicates a total of 2571 proteins detected in all three MDA-MB-231 shPIWIL4 samples. The *tan circle* (which also appears in three other different colors because of the overlap with the *blue* and *green circles*) indicates 7094 proteins that appear in at least one of the three MDA-MB-231 shPIWIL4 samples. *D*, reactome and KEGG pathway analysis from of 207 up-regulated proteins by an online tool, with $p < 0.0001$, which showed that components of the translational machinery are significantly enriched. *E*, reactome pathway analysis of 1288 down-regulated proteins by an online tool, with $p < 0.01$, which showed that the TGF-β and FGF signaling pathways are significantly enriched. *F*, TGFβR1, TGFβR2, FGFR2, TGFβ1, and TGFβ3 mRNA levels in the three PIWIL4 knockdown samples are down-regulated in three PIWIL4 knockdown cells compared with the control. *, $p < 0.05$; **, $p < 0.01$. *G*, gene ontology analysis of 1495 differentially expressed proteins by an online tool, with $p < 0.01$.

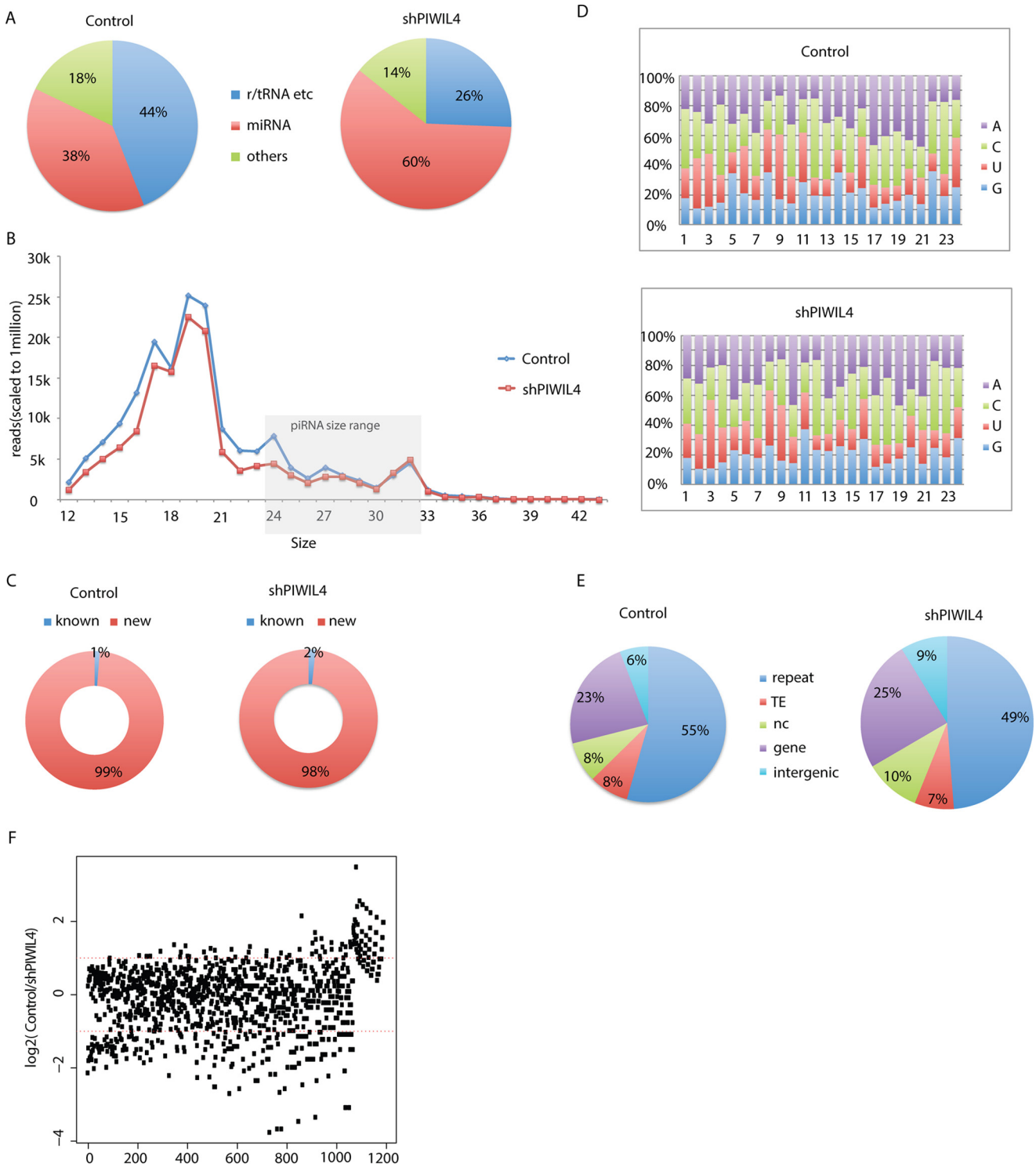

FIGURE 6. **Analysis of piRNAs in MDA-MB-231 cells.** *A*, pie chart illustrating the genomic source annotation of all mapped sequences. *B*, the size profile of the "others" group sequences. The 24- to 32-nt size range for putative piRNAs is shadowed in *gray*. The abundance was normalized to 1 million in each sample for comparison. *C*, donut display of known piRNAs (*known*) *versus* putative piRNAs (*new*) in the 24- to 32-nt population from the "others" group. *D*, nucleotide preference profile of 24- to 32-nt putative RNAs from position 1 to position 24. *E*, annotation of putative RNAs from the "others" group. *nc*, noncoding; *TE*, transposons. *F*, scatter plot of the ratio of all newly identified known and putative RNAs that had at least 10 mappable reads in either normal or PiwiL4 knockdown MDA-MB-231 cells. *Red dashed lines* correspond to log2 value 1, −1.

might repress MHC class II, which might help cancer cells avoid immune recognition (38, 39).

MDA-MB-231 Cells Express a Small Number of piRNAs—As the first step to investigate whether PIWIL4 function in MDA-MB-231 cells is related to piRNA, we examined whether these cells express piRNAs under normal PIWIL4 expression and PIWIL4 knockdown conditions. We isolated small RNA (12–42 nucleotides in length) from these cells with or without shPIWIL4 knockdown, followed by RT-PCR and deep sequencing. We observed the presence of many small RNAs in MDA-

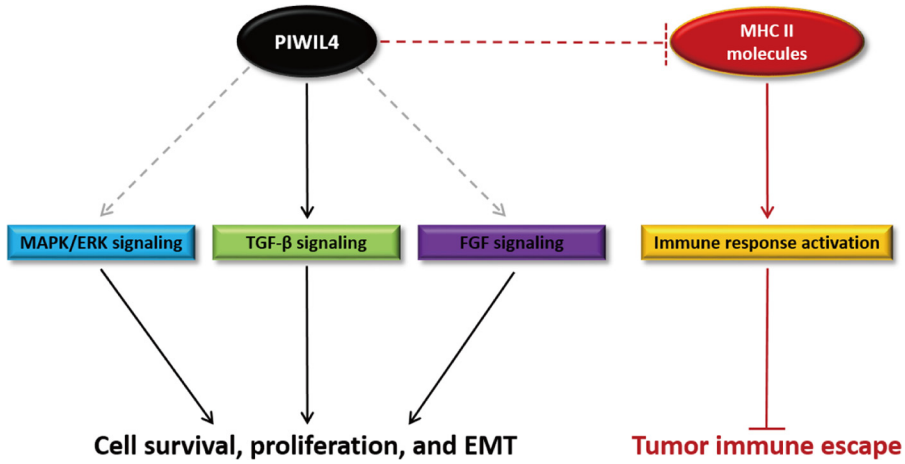

FIGURE 7. **A proposed regulation mechanism of PIWIL4 in the breast cancer cell line MDA-MB-231.** PIWIL4 could promote breast cancer cell survival, proliferation, epithelial-to-mesenchymal transition (*EMT*), and migration by activation of the TGF-*β*, FGF, and MAPK/ERK signaling pathways. Meanwhile, PIWIL4 might repress MHC class II, which helps cancer cells avoid immune recognition and reaction.

MB-231 cells under both conditions. These include miRNAs, other small RNAs, and fragments of rRNAs and tRNAs peaked at 19-nucleotide length (Figs. 6, *A* and *B*). Interestingly, under the knockdown condition, the miRNA population become significantly enriched in abundance (from 38% to 60% of the total small RNA reads, reflecting a 58% increase) at the expense of rRNA and tRNA fragments. Although this change could be due to less degradation of rRNA and tRNA in the RNA preparation from the PIWIL4 knockdown cells, this possibility is unlikely because, if so, the "other small RNA" fraction should correspondingly show a 58% increase in its abundance. However, the other small RNA fraction is decreased from 18% to 14%, reflecting a 29% decrease. Therefore, the increase in miRNA abundance mostly, if not exclusively, reflects a role of PIWIL4 in repressing miRNA expression in MDA-MB-231 cells.

To search for piRNAs, we selected small RNAs in the piRNA size range (24–32 nucleotides) for further analysis. Totally, 98,139 species of small RNAs are in this fraction from MDA-MB-231 cells without PIWIL4 knockdown and 55,624 species in this fraction from these cells with PIWIL4 knockdown. Among them, 61 species have previously been reported as human piRNAs (piRNABank and piRBase), with 50 and 53 species present in the normal and PIWIL4 knockdown MDA-MB-231 cells, respectively, representing 1% and 2% of the total small RNAs from the normal and knockdown cells (Fig. 6*C*).

The identification of these known piRNAs allowed us to conclude with reasonable confidence that at least some of the remaining 24- to 32-nucleotide small RNAs are piNRAs. However, these small RNA do not show the enrichment at either the 5′ first position for U that is a signature of primary piRNA or at the 5′ 10th position for A that is a signature of secondary piRNA (Fig. 6*D*). This could reflect that some of the small RNAs are not piRNAs. Alternatively, the signature may not be obvious because of the small number of species. To further search for sequence features of these small RNAs that may help us distinguish between the two possibilities, we mapped these small RNAs to the genome and found that they correspond to DNA repeats, transposons, intergenic sequences, and genes at proportions one would expect from piRNAs (Fig. 6*E*). These analyses support our conclusion that at least some of the small RNAs are likely piRNAs. Without experimental validation of their true identification, we can only call these small RNAs putative piRNAs. Combined data on the known piRNAs and putative piRNAs indicate that the MDA-MB-231 cells express a small number of piRNAs.

To assess how much of the expression of the putative piRNAs is affected by PIWIL4 knockdown, we first examined 24 known piRNAs (of the 61 known ones) that have at least 10 mappable reads in either normal or knockdown samples. Only three have a 2-fold or more decrease in PIWIL4 knockdown cells, and only one has a more than 2-fold increase, colored in red and blue, respectively, in supplemental Table S8. We then examined putative piRNAs with at least 10 mappable reads in both types of the cells. Of 1192 such piRNA candidates, only 333 show 2-fold or greater changes in abundance (Fig. 6*F*). These combined data on the known piRNAs and putative piRNAs indicate that the piRNA expression is not much affected by reducing the PIWIL4 level.

Discussion

PIWI proteins have been reported to be ectopically expressed in diverse types of cancer (17–21). However, most of these studies are at a correlative level. The role of PIWI expression in cancer remains unclear. Here we reported that PIWIL4 is widely expressed in breast cancer samples from different patients and in multiple breast cancer cell lines. Moreover, using a TNBC line (MDA-MB-231) as a model, we demonstrated that PIWIL4 expression promotes cancer cell survival, division, and, more significantly, migration. Our study provides a definitive demonstration of the function of PIWI proteins in cancer cells.

Furthermore, our transcriptome analysis revealed that PIWIL4 achieves its function in the breast cancer cells partially by activating TGF-*β*, MAPK/ERK, and FGF signaling and repressing MHC class II expression (Fig. 7). The TGF-*β*, FGF, and MAPK-ERK pathways are well known to play key roles in cancer. Specifically, TGF*β*R1 and TGF*β*R2 are known as receptors of TGF and other signaling molecules. They then activate downstream signal molecules during epithelial-to-mesenchymal transition of tumor cells (40). Some researchers suggested

that the expression of FGF4 and FGFR2 in ovarian cancer stem-like cells/cancer-initiating cells promoted their tumor initiation capacity (41). Our mass spectrometry results show that PIWIL4 promotes the TGF-β and FGF signaling pathways in the breast cancer cell line MDA-MB-231, which links PIWIL4 function to these important signaling pathways. In addition, our transcriptome analysis demonstrates that PIWIL4 also upregulates the MAPK-ERK signaling pathway (supplemental Fig. S4*A*). These findings reveal a new dimension of regulation of TGFβ and FGF signaling in cancer formation. The PIWIL4 regulation of these classic cancer signaling pathways provides an intellectual framework for further investigation of how PIWIL4 promotes breast cancer cell migration, survival, and proliferation through these pathways.

It is intriguing to see that PIWIL4 also suppress the expression of MHC class II genes. Tumorigenesis is a complex process involving not only signaling but also tumor immune escape pathways. MHC class II molecules are constitutively expressed in professional antigen-presenting cells, which is an essential part of cell-mediated immunity, but may also be induced on other cells by interferon γ (42). The suppression of MHC class II genes might help cancer cells avoid immune recognition and reaction by the T cell pathway.

PIWI proteins have multiple roles in the piRNA pathway. They participate in piRNA biogenesis in germ cells and represses transposon activity by affecting local epigenetic states and transcription (4). Correspondingly, piRNAs have important roles in mRNA regulation in the mouse by rendering targeting specificity (6, 43). Furthermore, some previous researchers suggested that piRNAs have independent functions, such as piR-823 having a role in breast cancer (5). Our analysis indicates that a small number of piRNAs are expressed in MDA-MB-231 cells. This raised the possibility that PIWIL4 works with piRNA to achieve its function. Further isolation of the PIWIL4-piRNA complex, identification of their regulatory targets, and analysis of their regulatory effect on the targets should shed light on how PIWI-mediated mechanisms function in cancer development.

Author Contributions—H. L. conceived the project. H. L., S. L., Z. W., and S. S. designed the experiments. Z. W. conducted most experiments. S. S. conducted some of the pilot experiments. H. L. and S. L. supervised the experiments. Z. W., S. L., and H. L. analyzed the data. N. L. conducted the bioinformatics analysis of piRNAs and mass spectrometry data. Z. W., S. L., N. L., and H. L. wrote the manuscript.

Acknowledgments—We thank Zhaoran Zhang for technical assistance, Drs. Chunchun Liu and Lishuang Zhang (SIAIS Flow Cytometry Platform) for assistance with cell sorting, Dr. Wei Zhu (SIAIS Mass Spectrometry Platform) for help with total cellular mass spectrometry, and Yingying Zhao (SIAIS Confocal Platform) for assistance with confocal imaging. We also thank the members of the Lin laboratory (ShanghaiTech University) for discussions and support.

References

1. Aravin, A., Gaidatzis, D., Pfeffer, S., Lagos-Quintana, M., Landgraf, P., Iovino, N., Morris, P., Brownstein, M. J., Kuramochi-Miyagawa, S., Nakano, T., Chien, M., Russo, J. J., Ju, J., Sheridan, R., Sander, C., *et al.* (2006) A novel class of small RNAs bind to MILI protein in mouse testes. *Nature* **442,** 203–207
2. Girard, A., Sachidanandam, R., Hannon, G. J., and Carmell, M. A. (2006) A germline-specific class of small RNAs binds mammalian Piwi proteins. *Nature* **442,** 199–202
3. Grivna, S. T., Beyret, E., Wang, Z., and Lin, H. (2006) A novel class of small RNAs in mouse spermatogenic cells. *Genes Dev.* **20,** 1709–1714
4. Juliano, C., Wang, J., and Lin, H. (2011) Uniting germline and stem cells: the function of Piwi proteins and the piRNA pathway in diverse organisms. *Annu. Rev. Genet.* **45,** 447–469
5. Yan, H., Wu, Q. L., Sun, C. Y., Ai, L. S., Deng, J., Zhang, L., Chen, L., Chu, Z. B., Tang, B., Wang, K., Wu, X. F., Xu, J., and Hu, Y. (2015) piRNA-823 contributes to tumorigenesis by regulating *de novo* DNA methylation and angiogenesis in multiple myeloma. *Leukemia* **29,** 196–206
6. Watanabe, T., and Lin, H. (2014) Posttranscriptional regulation of gene expression by Piwi proteins and piRNAs. *Mol. Cell* **56,** 18–27
7. Sytnikova, Y. A., Rahman, R., Chirn, G. W., Clark, J. P., and Lau, N. C. (2014) Transposable element dynamics and PIWI regulation impacts lncRNA and gene expression diversity in *Drosophila* ovarian cell cultures. *Genome Res.* **24,** 1977–1990
8. Yin, H., and Lin, H. (2007) An epigenetic activation role of Piwi and a Piwi-associated piRNA in *Drosophila melanogaster*. *Nature* **450,** 304–308
9. Lin, H., and Spradling, A. C. (1997) A novel group of pumilio mutations affects the asymmetric division of germline stem cells in the *Drosophila* ovary. *Development* **124,** 2463–2476
10. Cox, D. N., Chao, A., and Lin, H. (2000) piwi encodes a nucleoplasmic factor whose activity modulates the number and division rate of germline stem cells, *Development* **127,** 503–514
11. Deng, W., and Lin, H. (2002) miwi, a murine homolog of piwi, encodes a cytoplasmic protein essential for spermatogenesis. *Dev. Cell* **2,** 819–830
12. Kuramochi-Miyagawa, S., Kimura, T., Ijiri, T. W., Isobe, T., Asada, N., Fujita, Y., Ikawa, M., Iwai, N., Okabe, M., Deng, W., Lin, H., Matsuda, Y., and Nakano, T. (2004) Mili, a mammalian member of piwi family gene, is essential for spermatogenesis. *Development* **131,** 839–849
13. Carmell, M. A., Girard, A., van de Kant, H. J., Bourc'his, D., Bestor, T. H., de Rooij, D. G., and Hannon, G. J. (2007) MIWI2 is essential for spermatogenesis and repression of transposons in the mouse male germline. *Dev. Cell* **12,** 503–514
14. Gonzalez, J., Qi, H., Liu, N., and Lin, H. (2015) Piwi is a key regulator of both somatic and germline stem cells in the *Drosophila* testis. *Cell Rep.* **12,** 150–161
15. Cox, D. N., Chao, A., Baker, J., Chang, L., Qiao, D., and Lin, H. (1998) A novel class of evolutionarily conserved genes defined by piwi are essential for stem cell self-renewal. *Genes Dev.* **12,** 3715–3727
16. Lee, E. J., Banerjee, S., Zhou, H., Jammalamadaka, A., Arcila, M., Manjunath, B. S., and Kosik, K. S. (2011) Identification of piRNAs in the central nervous system. *RNA* **17,** 1090–1099
17. Kwon, C., Tak, H., Rho, M., Chang, H. R., Kim, Y. H., Kim, K. T., Balch, C., Lee, E. K., and Nam, S. (2014) Detection of PIWI and piRNAs in the mitochondria of mammalian cancer cells. *Biochem. Biophys. Res. Commun.* **446,** 218–223
18. Chen, C., Liu, J., and Xu, G. (2013) Overexpression of PIWI proteins in human stage III epithelial ovarian cancer with lymph node metastasis. *Cancer Biomark.* **13,** 315–321
19. Suzuki, R., Honda, S., and Kirino, Y. (2012) PIWI Expression and Function in Cancer. *Front. Genet.* **3,** 204
20. Wang, Y., Liu, Y., Shen, X., Zhang, X., Chen, X., Yang, C., and Gao, H. (2012) The PIWI protein acts as a predictive marker for human gastric cancer. *Int. J. Clin. Exp. Pathol.* **5,** 315–325
21. Siddiqi, S., and Matushansky, I. (2012) Piwis and piwi-interacting RNAs in the epigenetics of cancer. *J. Cell. Biochem.* **113,** 373–380
22. Qiao, D., Zeeman, A. M., Deng, W., Looijenga, L. H., and Lin, H. (2002) Molecular characterization of hiwi, a human member of the piwi gene family whose overexpression is correlated to seminomas. *Oncogene* **21,** 3988–3999
23. Ross, R. J., Weiner, M. M., and Lin, H. (2014) PIWI proteins and PIWI-interacting RNAs in the soma. *Nature* **505,** 353–359

24. Ye, Y., Yin, D. T., Chen, L., Zhou, Q., Shen, R., He, G., Yan, Q., Tong, Z., Issekutz, A. C., Shapiro, C. L., Barsky, S. H., Lin, H., Li, J. J., and Gao, J. X. (2010) Identification of Piwil2-like (PL2L) proteins that promote tumorigenesis. *PloS ONE* **5,** e13406
25. Linn, S. C., and Van 't Veer, L. J. (2009) Clinical relevance of the triple-negative breast cancer concept: genetic basis and clinical utility of the concept. *Eur. J. Cancer* **45,** 11–26
26. Rakha, E. A., and Ellis, I. O. (2009) Triple-negative/basal-like breast cancer: review. *Pathology* **41,** 40–47
27. Rakha, E. A., Elsheikh, S. E., Aleskandarany, M. A., Habashi, H. O., Green, A. R., Powe, D. G., El-Sayed, M. E., Benhasouna, A., Brunet, J. S., Akslen, L. A., Evans, A. J., Blamey, R., Reis-Filho, J. S., Foulkes, W. D., and Ellis, I. O. (2009) Triple-negative breast cancer: distinguishing between basal and nonbasal subtypes. *Clin. Cancer Res.* **15,** 2302–2310
28. Liedtke, C., Mazouni, C., Hess, K. R., André, F., Tordai, A., Mejia, J. A., Symmans, W. F., Gonzalez-Angulo, A. M., Hennessy, B., Green, M., Cristofanilli, M., Hortobagyi, G. N., and Pusztai, L. (2008) Response to neoadjuvant therapy and long-term survival in patients with triple-negative breast cancer. *J. Clin. Oncol.* **26,** 1275–1281
29. Banerji, S., Cibulskis, K., Rangel-Escareno, C., Brown, K. K., Carter, S. L., Frederick, A. M., Lawrence, M. S., Sivachenko, A. Y., Sougnez, C., Zou, L., Cortes, M. L., Fernandez-Lopez, J. C., Peng, S., Ardlie, K. G., Auclair, D., *et al.* (2012) Sequence analysis of mutations and translocations across breast cancer subtypes. *Nature* **486,** 405–409
30. Koboldt, D. C., Fulton, R. S., McLellan, M. D., Schmidt, H., Kalicki-Veizer, J., McMichael, J. F., Fulton, L. L., Dooling, D. J., Ding, L., Mardis, E. R., Wilson, R. K., Ally, A., Balasundaram, M., Butterfield, Y. S. N., Carlsen, R., *et al.* (2012) Comprehensive molecular portraits of human breast tumours. *Nature* **490,** 61–70
31. Lehmann, B. D., Bauer, J. A., Chen, X., Sanders, M. E., Chakravarthy, A. B., Shyr, Y., and Pietenpol, J. A. (2011) Identification of human triple-negative breast cancer subtypes and preclinical models for selection of targeted therapies. *J. Clin. Invest.* **121,** 2750–2767
32. Shah, S. P., Morin, R. D., Khattra, J., Prentice, L., Pugh, T., Burleigh, A., Delaney, A., Gelmon, K., Guliany, R., Senz, J., Steidl, C., Holt, R. A., Jones, S., Sun, M., Leung, G., *et al.* (2009) Mutational evolution in a lobular breast tumour profiled at single nucleotide resolution. *Nature* **461,** 809-U867
33. Soufla, G., Sifakis, S., Baritaki, S., Zafiropoulos, A., Koumantakis, E., and Spandidos, D. A. (2005) VEGF, FGF2, TGFB1 and TGFBR1 mRNA expression levels correlate with the malignant transformation of the uterine cervix. *Cancer Lett.* **221,** 105–118
34. Marek, L., Ware, K. E., Fritzsche, A., Hercule, P., Helton, W. R., Smith, J. E., McDermott, L. A., Coldren, C. D., Nemenoff, R. A., Merrick, D. T., Helfrich, B. A., Bunn, P. A., Jr., and Heasley, L. E. (2009) Fibroblast growth factor (FGF) and FGF receptor-mediated autocrine signaling in non-small-cell lung cancer cells. *Mol. Pharmacol.* **75,** 196–207
35. Lee, J. H., Jung, C., Javadian-Elyaderani, P., Schweyer, S., Schütte, D., Shoukier, M., Karimi-Busheri, F., Weinfeld, M., Rasouli-Nia, A., Hengstler, J. G., Mantilla, A., Soleimanpour-Lichaei, H. R., Engel, W., Robson, C. N., and Nayernia, K. (2010) Pathways of proliferation and antiapoptosis driven in breast cancer stem cells by stem cell protein Piwil2. *Cancer Res.* **70,** 4569–4579
36. Cerami, E., Gao, J., Dogrusoz, U., Gross, B. E., Sumer, S. O., Aksoy, B. A., Jacobsen, A., Byrne, C. J., Heuer, M. L., Larsson, E., Antipin, Y., Reva, B., Goldberg, A. P., Sander, C., and Schultz, N. (2012) The cBio Cancer Genomics Portal: an open platform for exploring multidimensional cancer genomics data. *Cancer Discov.* **2,** 401–404
37. Gao, J., Aksoy, B. A., Dogrusoz, U., Dresdner, G., Gross, B., Sumer, S. O., Sun, Y., Jacobsen, A., Sinha, R., Larsson, E., Cerami, E., Sander, C., and Schultz, N. (2013) Integrative Analysis of complex cancer genomics and clinical profiles using the cBioPortal. *Sci. Signal.* **6,** pl1
38. Meazza, R., Comes, A., Orengo, A. M., Ferrini, S., and Accolla, R. S. (2003) Tumor rejection by gene transfer of the MHC class II transactivator in murine mammary adenocarcinoma cells. *Eur. J. Immunol.* **33,** 1183–1192
39. Mottok, A., Woolcock, B., Chan, F. C., Tong, K. M., Chong, L., Farinha, P., Le Telenius, A., Chavez, E., Ramchandani, S., Drake, M., Boyle, M., Ben-Neriah, S., Scott, D. W., Rimsza, L. M., Siebert, R., *et al.* (2015) Genomic alterations in CIITA are frequent in primary mediastinal large B cell lymphoma and are associated with diminished MHC class II expression. *Cell Rep.* **13,** 1418–1431
40. Zavadil, J., and Böttinger, E. P. (2005) TGF-β and epithelial-to-mesenchymal transitions. *Oncogene* **24,** 5764–5774
41. Yasuda, K., Torigoe, T., Mariya, T., Asano, T., Kuroda, T., Matsuzaki, J., Ikeda, K., Yamauchi, M., Emori, M., Asanuma, H., Hasegawa, T., Saito, T., Hirohashi, Y., and Sato, N. (2014) Fibroblasts induce expression of FGF4 in ovarian cancer stem-like cells/cancer-initiating cells and upregulate their tumor initiation capacity. *Lab. Invest.* **94,** 1355–1369
42. Ting, J. P., and Trowsdale, J. (2002) Genetic control of MHC class II expression. *Cell* **109,** S21–33
43. Watanabe, T., Cheng, E. C., Zhong, M., and Lin, H. (2015) Retrotransposons and pseudogenes regulate mRNAs and lncRNAs via the piRNA pathway in the germline. *Genome Res.* **25,** 368–380